Lithuanian Journal of Physics, Vol. **44**, No. 5, pp. 329–336 (2004)

FORMATION OF AMORPHOUS CARBON FILMS IN PLASMA OF HYDROGEN AND HYDROCARBON MIXTURES

A. Grigonis [a], Ž. Rutkūnienė [a], and M. Šilinskas [b]

[a] *Physics Department, Kaunas University of Technology, Studentų 50, LT-51368 Kaunas, Lithuania*
[b] *Institute of Micro- and Sensor Systems, Otto von Guericke University, Universitätsplatz 2, 39106 Magdeburg, Germany*

Received 05 May 2004

Dedicated to the 100th anniversary of Professor K. Baršauskas

Deposition of amorphous hydrogenated carbon (a-C:H) films in CF_4, hexane (C_6H_{14}), or acetylene (C_2H_2) precursors and their mixtures with hydrogen (H_2) is reported. The films were characterized by Raman spectroscopy (RS) and X-ray spectroscopy (XPS). RS indicates increase of the sp^3/sp^2 bonding ratio and disorder in graphite clusters with increasing hydrogen content (from 0 to 50% for the acetylene precursor) in the deposition gas mixture. The opposite trend is observed when the hydrogen concentration exceeds 50% (for acetylene) or additional hydrogen is used (for hexane). Formation of polymer-like films in fluorine-containing gas plasma is observed with additional low quantity of hydrogen (~5%). Composition of these films depends on treatment duration and conditions of irradiation.

Keywords: amorphous carbon films, Raman spectroscopy, X-ray photoelectron spectroscopy

PACS: 78.30.–j, 81.07.Bc, 81.15.Ij

1. Introduction

Amorphous carbon films, because of their unique optical, mechanical, electrochemical properties, are used for many applications, such as mechanical, electronic, optical, and biomedical [1–5].

Unlike amorphous Si and Ge, amorphous carbon forms sp^3, sp^2, and sp^1 bonds. Depending on the predominant type of bonds, amorphous carbon films are:

(a) diamond-like (DLC) films, where the predominant bonds are sp^3, and their mechanical strength, band gap, refraction index, thermal and electrical conductivity may vary in a wide interval;
(b) graphite-like carbon (GLC) films, where the predominant bonds are sp^2, and they are soft, conductive, often obtained as nanocrystalline formation (fullerenes, nanotubes, nanocones, etc.);
(c) polymer-like carbon (PLC) films, and they are soft, with wide band gap, having high concentration of hydrogen.

Additional impurities like hydrogen, silicon, nitrogen, fluorine, boron, and other can modify the properties of all these films.

a-C:H films are amorphous in nature with no long-range crystallinity and high hydrogen concentration. Robertson [4–6] proposed the cluster model, and predicted that sp^2 sites form clusters embedded in an sp^3-bonded matrix. The range of cluster sizes is large, but usually sp^2 islands are limited to single sixfold rings (aromatic) and short chains (olefinic) [6]. The properties of plasma-deposited a-C:H films are determined by the carbon sp^3/sp^2 bonding ratio and by the hydrogen content [7]]. Hydrogen appears to play a very significant role [4, 8–10]. Hydrogen can increase the fraction of C–C sp^3 and C–H bonding. Paterson [11, 12] investigated the influence of hydrogen in direct ion beam deposition from methane but it is unclear for other hydrocarbon gases. Schwartz-Selinger et al. [7] found that a-C:H film properties depended on the hydrocarbon source and hydrogen content using ion-beam-assisted deposition without heating. The same conclusion was made for electron-beam-excited plasma CVD by Ban et al. [10]. A framework for understanding a-C:H film growth was given by Jakob [13].

Raman spectroscopy (RS) has been widely used for the characterization of the carbon films [3, 4, 10]. It has been reported that a-C:H films have a broad asymmetrical peak in the 1100–1700 cm^{-1} range and it may have two shoulders at 1570 and 1350 cm^{-1}. These peaks have been abbreviated as the G and D band, respec-

© Lithuanian Physical Society, 2004
© Lithuanian Academy of Sciences, 2004
ISSN 1648-8504

tively. Both these peaks are due to sp^2 sites. The effect of sp^3 sites is mainly via their influence on the sp^2 configuration. Changes in the G peak position and width (γ_G) are associated with changes in the amount of disorder in the sp^2-bonded fraction of a-C:H. The D peak position correlates with the proportion of sp^3-bonded carbon present. The D and G peak intensity ratio I_D/I_G is associated with the sp^3/sp^2 bonding ratio and the size of graphite clusters [4, 11].

In previous works [15, 16], we investigated the a-C:H films deposited from the mixture of hexane and hydrogen gases. It has been found that the properties of carbon films depend on ion energy, temperature, and silicon content. The best diamond-like films were obtained at lower temperatures (at room temperature) and lower ion energy (600 eV). We also found that the carbon film structure correlated with hydrogen content in the gas mixture at low temperature ($\sim$15 °C). In this work, we continue to study hydrogen influence on the carbon film properties in the direct ion beam deposition process.

Halogen-containing carbon plasmas are widely used as reactive etching plasmas in micro- and optical electronics for formation of micron and submicron structures. Ion bombardment is responsible for the etching anisotropy, and active radicals for the etching rate and selectivity. In the case of polycomponent plasma, ion-assisted etching is also accompanied with ion-assisted deposition that is associated with polymerization of CF_x, CH_x, C–CF_x ($x > 2$) radicals in the fluorine carbon plasmas (CF_4, C_3F_8, especially with hydrogen mixing $CF_4 + H_2$, CF_2HCl). The etching in the pure CF_4 gas plasma is isotropic but with etching duration the concentration on the surface increases and interrupts this process [14]. The mixture of hydrogen with CF_4 gas results in deficiency of fluorine atoms in plasma. It gives increase in the concentration of CF_2, CHF_2, and other monomers that have unsaturated bonds in the gaseous phase and may easily form a polymeric layer on the surface, and this can be a condition for getting the polymer-like films.

2. Experiment

Polymer-like carbon films were formed on single-crystal p-type 4.5 Ω·cm silicon (111) substrates in CF_4, $CF_4 + H_2$ gases in a 13.6 MHz asymmetric diode system PK 2420 RIE (ADS), where the samples had a negative bias voltage (0.1–0.5 keV), and pressure could be varied (0.1–26.6 Pa). The cathode diameter was 0.1 m, the vacuum chamber diameter 0.88 m, its height 0.34 m, and a pumping system MPB-35 was used in the PK 2420 RIE system. The ion energy was derived from DC negative bias voltage expressed in eV.

Diamond-like a-C:H films were also deposited on Si(100) and (111) to a thickness up to 400 nm by applying the direct ion beam deposition method at 15–2000 °C temperature. Further details are reported elsewhere [17]. The films were formed from the following gas mixtures: (a) hexane (C_6H_{14}), (b) hexane and hydrogen, (c) acetylene, (d) acetylene and hydrogen. The hexane was delivered from liquid phase by the same hydrogen flow. The ion energy was 1000 eV, ion current density $\sim$0.12 mA/cm^2, pressure below 10^{-2} Pa, deposition durations were 30 and 90 min.

The composition of the altered layer was subsequently analysed *ex situ* by X-ray photoelectron spectroscopy (XPS) (spectrometer KRATOS ANALYTICAL), ellipsometry (variable angle null ellipsometer EL11D, wavelength 632.8 nm, He–Ne laser), and Raman spectroscopy.

RS measurements were performed under the argon laser irradiation of 514.5 nm wavelength and 20 mW excitation power at a 2 mm spot size. Data were collected in backscattering geometry at room temperature. Distribution curves were fitted with the same Gaussian shapes at a linear background using the least squares fitting software. Raman spectra were taken in the range of 400–2000 cm^{-1}, but fitting was performed only for the 1000–1800 cm^{-1} range.

XPS spectra were obtained using an Al K_α radiation source. XPS spectra were separated into components by the least squares method in order to estimate the binding energy and photoelectron intensity of each component. Type of bonds was estimated from the previous reports [18–21].

A steady-state condition on the surface occurs some 20–40 min after the interruption of the etching process and depends on the adsorption of admixtures from the surroundings.

3. Results and discussion

3.1. a-C:H films formation in CF_4 and $CF_4 + H_2$ plasma

Surface carbon concentration is measurable when silicon is etched in CF_4 plasma, and addition of oxygen (10%) has not stopped accumulation of it. XPS measurements have shown that the width and mean of the C $1s$ peak depend on the ion energy. The peak

Table 1. Type and concentration of carbon bonds after treatment of the silicon surface in $CF_4 + 5\%$ H_2 plasma.

Etching duration, min	C–C	$(CH_2)_n$	C–CF_x	C–F	$(CHFCHF)_n$
5	65	13	6	13	0
10	49	0.7	30	10	13
20	43	0	44	11	0

maximum is in the binding energy interval of 284.6–285 eV when the ion energy is $E_{\mathrm{i}} = 0.7-1$ keV. It means that carbon is unbound or is in the SiC bonds. The peak maximum is shifted to the higher-energy side (0.5–1 eV) when the ion energy decreases ($E_{\mathrm{i}} <$ 0.5 keV). So, carbon exists in the bonds with oxygen (C–O–C, C–O) and unbounded carbon is obtained on the surface, and it is correct, because less ions penetrate into the crystal bulk when the ion energy decreases. But accumulation of a thin amorphous and porous carbon layer has not interrupted the etching.

Addition of 5% of hydrogen in the CF_4 plasma stimulates condensation of polymeric compounds on the silicon surface (Table 1). From XPS spectra we obtained that carbon, silicon, hydrogen, fluorine, and oxygen are present in the composition of the formed film. Oxygen is only on the film surface – it is adsorbed from surroundings (XPS measurements going *ex situ*). As a result, we have obtained that a thin film of α-Si_xC_{1-x}:H:F of variable composition and complicated structure is formed on the silicon surface. As measurements show, etching velocity depends on the surface carbon state. After 10 min of etching it has been obtained from XPS C $1s$ spectra that carbon can create the following kinds of bonds: C–CF_x (30%), C–C or C–H (47%), and it can be in the composition of $(CHFCH_2)_n$ compounds. The dependence of carbon bonds on etching duration was analysed [14] and it was obtained that not only carbon in C–CF_x bonds became predominant, but also fluorine concentration increased there when etching duration increased. The state of surface carbon also depends on the hydrogen concentration in plasma, discharge power density, and etching duration [14]. The concentration of $(CH_2)_n$ and $(CHFCH_2)_n$ bonds decreased with increasing the discharge power density and ion energy. The peak of C $1s$ shifted to the higher-energy side and it meant that $(C\text{–}CF_2)_n$ stable inhibitor had formed on the surface.

After the analysis of RS spectra (Fig. 1) it was obtained that the formed film was amorphous and had a high concentration of impurities. Several peaks had the following characteristics: 519 cm^{-1} (silicon substrate conditioned it and the peak showed that the film was transparent), 1160 cm^{-1} (in our opinion, it belonged

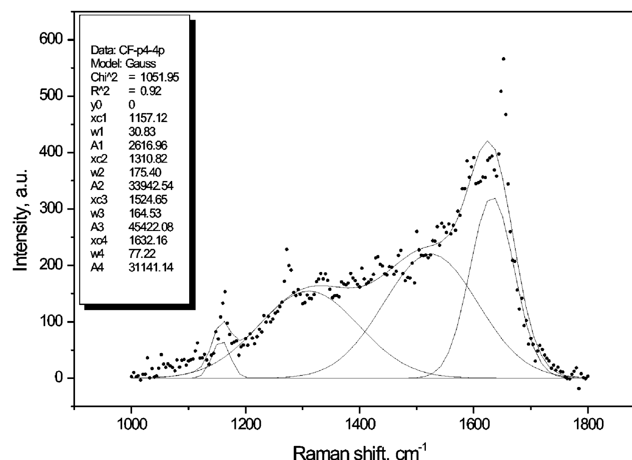

Fig. 1. Typical RS spectra after silicon etching in $CF_4 + H_2$ plasma.

to a single C–C bond with C–H trend, but other authors attributed it to nanocrystaline 1–100 nm carbon formation and related it with the small size of crystallites or/and with disorder in the tetrahedron structure [15, 16]). Typical DLC lines are substantially shifted to the lower-energy side: D line to 1274 cm^{-1} and G line to 1430 cm^{-1} after 10 min of etching in $CF_4 + 20\%$ H_2 plasma. Silicon impurities influenced it, because silicon concentration decreased from 20% (etching time 10 min) to 10–20% (etching time 40 min) with increasing the etching duration. The peak of the D line shifted by 13 cm^{-1}, while that of the G line by 31 cm^{-1}. Positions of peaks and their widths showed that the film was amorphous, but changes of carbon bonds in the film and quick removal of the graphite stage with active reagents (H, F) made the film more transparent – the peak of the silicon substrate increased.

3.2. a-C:H film formation in hexane ($C_6H_{14} + H_2$) or acetylene ($C_2H_2 + H_2$) and ($C_6H_{14} + H_2$) + H_2 mixture plasma

The film thickness decreases with an increase of hydrogen content in the deposition gas mixture. Table 2 contains the details of deposition in hexane and acetylene plasmas and their mixtures with hydrogen. When the hydrogen/hexane ratio is $3/1$ and the concentration of hydrogen is 86%, no film growth is observed.

Table 2. Film growth conditions.

Precursor	Transport gas	Precursor/H_2 ratio	T, °C	t, min	d, nm
C_6H_{14}	H_2	–	∼15	90	300
C_6H_{14}	H_2	1/1.5	∼15	90	280
C_6H_{14}	H_2	1/3	∼15	90	no deposition
C_2H_2	–	–	∼20	30	169
C_2H_2	–	1/0.5	∼20	30	105
C_2H_2	–	1/1	∼20	30	100
C_2H_2	–	1/2	∼20	30	70
C_2H_2	–	1/3	∼20	30	39
C_2H_2	–	1/5	∼20	30	no deposition
C_2H_2	–	1/10	∼20	30	no deposition

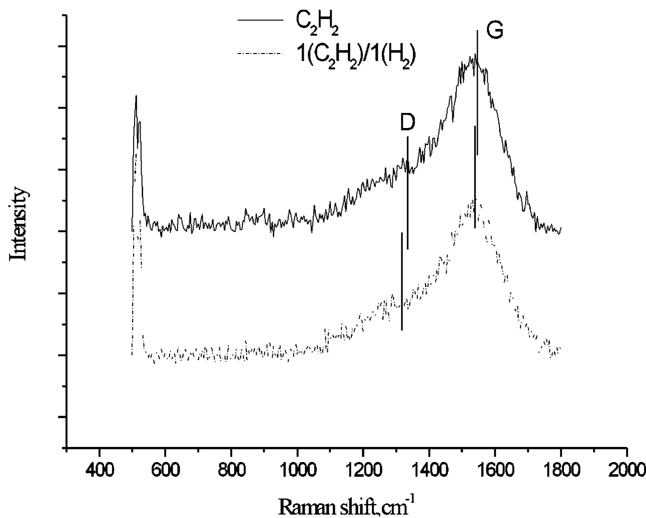

Fig. 2. Examples of Raman spectra of a-C:H (from acetylene) with and without additional hydrogen.

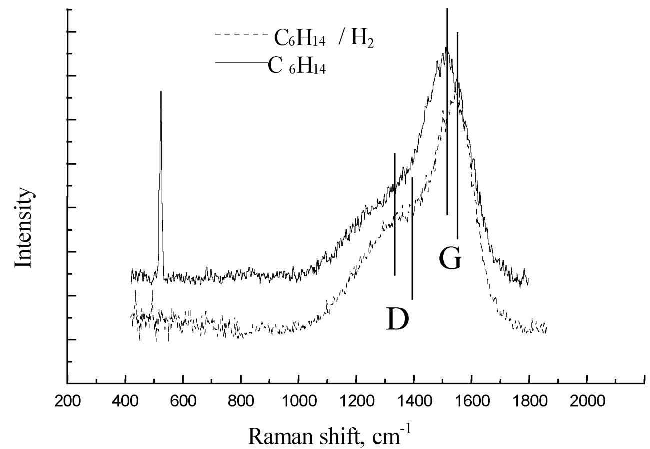

Fig. 3. Examples of Raman spectra of a-C:H (from C_6H_{14}) with and without additional hydrogen.

These results correlate with the similar work done by Paterson [11] where it has been found that deposition rates depend on the methane/hydrogen ratio, and for 90% H_2 in the feed gas, little or no film has been deposited. There only the total gas flow volume was measured and the author explained reduction of the deposition rate by decrease of the amount of the carbon-containing gas and by sputtering.

The film deposition behaviour indicates that the sputtering or etching process is faster than the deposition process for high hydrogen content. This suggestion is valid for many hydrocarbon gases and does not depend on hydrocarbon nature (CH_4 [11], C_6H_{14}, C_2H_2).

Raman spectra of carbon films are given in Figs. 2 and 3.

There is a broad asymmetrical carbon peak at 1500 cm^{-1} and a silicon peak at 521 cm^{-1}. The highest silicon peaks were observed when the acetylene/hydrogen ratio was 1/1 or only hexane was used. It means that these coatings are more transparent for laser light and contain less graphite component. It is also clear that the films deposited from acetylene are less sensitive to changes of the hydrogen concentration in the deposition gas mixture.

The Raman results for a-C:H films deposited using various acetylene/hydrogen mixtures are shown in Fig. 4. The G and D band positions (∼1544 and 1320 cm^{-1}) and the I_D/I_G ratio (∼0.6) are the lowest when the acetylene/hydrogen ratio is 1/1. The largest width (FWHM) of the G band (∼160 cm^{-1}) is at the same gas proportion. Because the D band width is too much scattered it has not been used. When only acetylene gas is used, the positions of G and D bands are at ∼1552 and ∼1345 cm^{-1}, respectively, their intensity ratio is about 1.0, and the G band width is 150 cm^{-1}. This indicates that additional hydrogen enhances fourfold coordinate bonding and makes length and angles order in graphite islands worse.

When the hydrogen/acetylene gas ratio is 1/1, the films are transparent in the range of 2.5–25 μm. But when the hydrogen content decreases to 33% the IR transmission spectra show absorption from 6 μm.

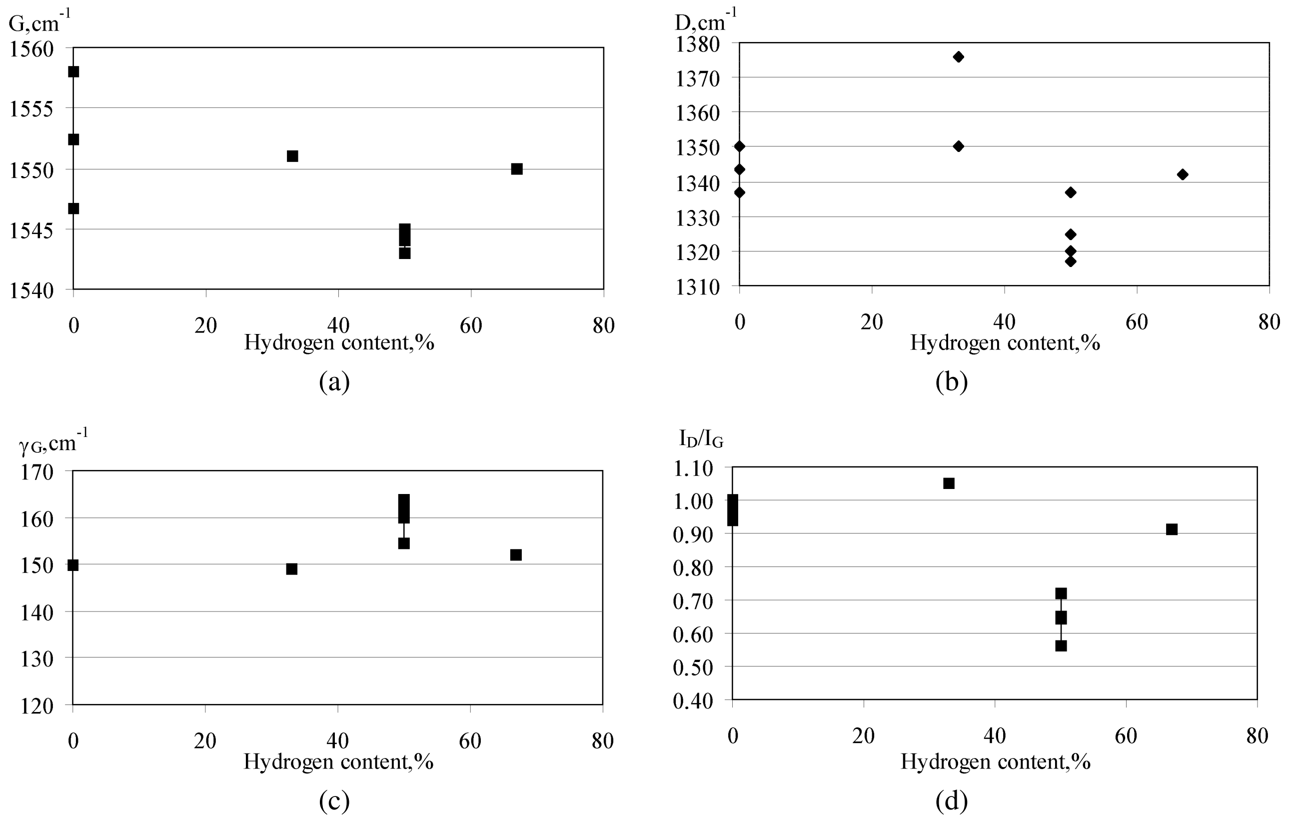

Fig. 4. The Raman data of a-C:H films deposited from various acetylene/hydrogen mixtures.

Table 3. Characteristics of Raman spectra of films deposited from hexane.

Precursor	Precursor/H_2 ratio	G, cm^{-1}	D, cm^{-1}	γ_G, cm^{-1}	I_D/I_G
C_6H_{14}	–	1530	1330	150	0.77
C_6H_{14}	1/1.5	1553	1376	122	1.48

When the concentration of hydrogen in the deposition gas mixture is 67% the G and D bands also shift to the higher wavenumber range (1555 and 1345 cm^{-1}), the I_D/I_G ratio increases (~0.9), and the G band gets narrow (152 cm^{-1}). In this case the changes of Raman features have not been so great. This means that the sp^3/sp^2 ratio and disorder in graphite islands increase but not so significantly as in the case without hydrogen. It has not been possible to obtain meaningful Raman data for films deposited with even higher hydrogen concentration because the film thickness has not been sufficient for RS. From these results it is clear that the best quality (closer to diamond-like) of the films deposited from the acetylene/hydrogen gas mixture are at 50% of hydrogen.

Table 3 shows the features of RS for carbon films deposited from hexane. The G and D band positions shift to higher energy (from 1530 and 1330 cm^{-1} to 1553 and 1376 cm^{-1} for G and D peaks, respectively), the G band width decreases (from 150 to 122 cm^{-1}) and the I_D/I_G ratio increases (from 0.77 to 1.48) with increasing hydrogen concentration in the deposition gas mixture. There was no maximum observed in the Raman features because hydrogen was used as delivery gas and it was impossible to get the deposition gas mixture without hydrogen. We also observed a reduced wear resistance with increasing hydrogen content [16]. In the case of hexane, the best quality of the films was achieved without additional hydrogen.

From these results it is clear that two hydrogen-related effects are observed. In the first range (≤50% of hydrogen for acetylene) there is a very small amount of hydrogen because the hydrogen/carbon ratio in the acetylene molecule is 1/1. In saturated hydrocarbon (hexane) this ratio is higher (~2.3). This difference is one reason why the RS measurements do not show any maximum for hexane. According to a framework for understanding a-C:H film growth proposed by Jacob [13], the carbon-carrying ions and neutral carbon-carrying radicals contribute to film growth. When we

add the additional hydrogen in the feed gas mixture, less hydrocarbon ions reach the substrate and the deposition rate decreases. In the case of radicals, the explanation is not very simple because the deposition rate depends not only on carbon-carrying radical concentration but also on dangling bonds density. The radicals chemisorb on dangling bonds at the surface, which are usually created by ion bombardment [18, 19]. When acetylene is used, the anticipated dominant precursor is the ethinyl radical (C_2H). This radical can also produce new dangling bonds if the hybridization is changed upon adsorption (from sp^1 to sp^2 or sp^3) [7]. On the other hand, atomic hydrogen can saturate dangling bonds, abstract bonded hydrogen, hydrogenate sp^2 groups. However, the contribution of abstracting bonded hydrogen and hydrogenating sp^2 sites to film growth is usually negligible, while energetic ions produce much more dangling bonds, and the dominant effect is the saturation of dangling bonds. Hence, the deposition rate decreases with increasing hydrogen content in the deposition gas mixture. But hydrogenation of sp^2 carbon–carbon double bonds at the surface and formation of sp^3 carbon groups [5, 9] decreases the amount of sp^2-bonded carbon, reduces the size and order of graphite clusters.

When the amount of hydrogen exceeds the critical concentration ($\geq$50% for acetylene), the RS and electrical resistivity measurements show a stronger graphite phase. It is possible that instead of C–C sp^3 bonds linear C–C sp^1 or C–H bonds are formed (reduced wear resistance) and the polymer-like carbon allows formation of better order in graphite islands. The polymer-like nature was observed in the earlier work [16] where a-C:H films were investigated by X-ray electron spectroscopy and mechanical measurements. It has been found that additional hydrogen can form various linear chains with hydrogen and oxygen instead of sp^3 bonds. In this hydrogen concentration range ($\geq$50% for acetylene), low deposition rate correlates with stronger graphite-like properties of a-C:H films determined by RS and electrical resistivity measurements. This correlation was observed by many authors [11, 23, 24]. Paterson [11] investigated this effect for lower acceleration potentials ($\leq$500 V). The author supposed that the increase in the sp^2 order was probably due to defect annealing processes. But there was not clear why the defects were not annealed when the hydrogen concentration was less than 80%. The theoretical prediction for this phenomenon was made by Jacob [13]. He calculated by TRIM.SP that the ratio of inelastic energy loss and elastic energy loss was much higher for hydrogen than for carbon. This is valid not only for the surface layer but also for almost all the penetration depth. The elastic collision is available for a nonequilibrium process and might increase the number of sp^3 bonds. The inelastic dissipated energy is rapidly converted to thermal energy, the defects in the graphite clusters anneal, and some of sp^3 bonds are converted to thermodynamically stable sp^2. When the defect annealing process becomes stronger than hydrogenation of sp^2 groups, we observe a decrease in electrical resistivity and RS shows a graphitization process. We should note that additional hydrogen in the gas mixture increases the hydrogen concentration in the a-C:H film [16, 22]. As a result, there is also a polymerization process and we obtain sp^2 islands in polymer-like carbon.

4. Conclusions

1. Films of various compositions grow in $CF_4 + H_2$ plasma. Carbon on the surface takes part in formation of polymeric $(C\text{–}CF_x)_n$, $(CH_2)_n$ compounds, but higher carbon concentrations are in C–C bonds that are characteristic of DLC type films.
2. The film growth rate decreases with increasing hydrogen content in $C_2H_2 + H_2$ and $C_6H_{14} + H_2$ plasma. The highest sp^3/sp^2 bonding ratio and higher disorder of graphite clusters are achieved when the hydrogen/acetylene ratio is $1/1$.
3. The highest sp^3/sp^2 bonding ratio and higher disorder of graphite clusters are achieved when no additional hydrogen is used in hexane plasma.
4. Inelastic dissipation energy increases the sp^2/sp^3 ratio and improves order in graphite clusters.

Acknowledgement

This work was partially supported by the Lithuanian State Science and Education Foundation.

References

[1] N. Gopinathan, C. Robinson, and F. Ryan, Characterization and properties of diamond-like carbon films for magnetic recording application, Thin Solid Films **355–356**, 401–405 (1999).

[2] L.Yu. Ostrovskaya, Studies of diamond and diamond-like film surfaces using XAES, AFM and wetting, Vacuum **68**(3), 219–238 (2002).

[3] C.L. Cheng, C.T. Chia, C.C. Chiu, and I.-N. Lin, Time-dependent *in-situ* Raman observation of atomic hydrogen etching on diamond-like carbon films, Diamond Relat. Mater. **11**(2), 262–267 (2002).

[4] J. Robertson, Requirements of ultrathin carbon coatings for magnetic storage technology, Tribology International **36**(4–6), 405–415 (2003).

[5] J. Robertson, Improving the properties of diamond-like carbon, Diamond Relat. Mater. **12**(2), 79–84 (2003).

[6] J. Robertson, Structural models of a-C and a-C:H, Diamond Relat. Mater. **4**(4), 297–301 (1995).

[7] T. Schwarz-Selinger, A. von Keudell, and W. Jakob, Plasma chemical vapor deposition of hydrocarbon films: The influence of hydrocarbon source gas on the film properties, J. Appl. Phys. **86**(7), 3988–3996 (1999).

[8] A. von Keudell, T. Schwarz-Selinger, and W. Jakob, Simultaneous interaction of methyl radicals and atomic hydrogen with amorphous hydrogenated carbon films, J. Appl. Phys. **89**(5), 2979–2986 (2001).

[9] A. von Keudell, T. Schwarz-Selinger, M. Meier, and W. Jacob, Direct identification of the synergism between methyl radicals and atomic hydrogen during growth of amorphous hydrogenated carbon films, Appl. Phys. Lett. **76**(6), 676–678 (2000).

[10] M. Ban, T. Hasegawa, S. Fujii, and J. Fujioka, Stress and structural properties of diamond-like carbon films deposited by electron beam excited plasma CVD, Diamond Relat. Mater. **12**(1), 47–56 (2003).

[11] M.J. Paterson, An investigation of the role of hydrogen in ion beam deposited a-C:H, Diamond Relat. Mater. **7**(6), 908–915 (1998).

[12] M.J. Paterson, Energy dependent structure changes in ion beam deposited a-C:H, Diamond Relat. Mater. **5**(12), 1407–1413 (1996).

[13] W. Jakob, Surface reactions during growth and erosion of hydrocarbon films, Thin Solid Films, **326**(1–2), 1–42 (1998).

[14] Ž. Rutkūnienė and A. Grigonis, Formation of polymeric layers using halogen–carbon plasmas, Vacuum **68**(3), 239–244 (2003).

[15] A. Grigonis, M. Silinskas, and V. Kopustinskas, Investigation of ion irradiation effects in a-Si_xC_{1-x}:H thin films, Vacuum **68**(3), 257–261 (2003).

[16] M. Silinskas and A. Grigonis, Low energy post-growth irradiation of amorphous hydrogenated carbon (a-C:H) films, Diamond Relat. Mater. **11**(3–6), 1026–1030 (2002).

[17] M. Silinskas, A. Grigonis, and H. Manikowski, Optical and electron paramagnetic resonance studies of hydrogenated amorphous carbon (a-C:H) thin films formed by direct ion beam deposition method, Proc. SPIE **4415**, 266–271 (2001).

[18] M. Horie, Plasma-structure dependence of the growth mechanism of plasma-polymerized fluorocarbon films with residual radicals, J. Vac. Sci. Technol. A **13**(5), 2490–2497 (1995).

[19] N. Hirashita, Y. Miyakawa, K. Fujita, and J. Kanamory, Reaction studies between fluorocarbon films and Si using temperature-programmed X-ray photoelectron and desorption spectroscopies, Jpn. J. Appl. Phys. **34**(4B), 2137–2141 (1995).

[20] Sh. Arai, K. Tsujimoto, and S. Tachi, Deposition in dry-etching gas plasmas, Jpn. J. Appl. Phys. **31**(6B), 2011–2019 (1992).

[21] *Practical Surface Analysis by Auger and X-Ray Photoelectron Spectroscopy*, eds. D. Brigs and M.P. Seach (UK, 1983) p. 589.

[22] C. Hopf, A. von Keudell, and W. Jacob, The influence of hydrogen ion bombardment on plasma-assisted hydrocarbon film growth, Diamond Relat. Mater. **12**(2), 85–89 (2003).

[23] A. von Keudell, W. Jacob, and C. Hopf, Growth mechanism of amorphous hydrogenated carbon, Diamond Relat. Mater. **11**(3–6), 969–975 (2002).

[24] J.L. Andujar, M. Vives, C. Corbella, and E. Bertran, Growth of hydrogenated amorphous carbon films in pulsed d.c. methane discharges, Diamond Relat. Mater. **12**(2), 98–104 (2003).

AMORFINIŲ ANGLIES DANGŲ SUDARYMAS VANDENILIO IR ANGLIAVANDENILIŲ MIŠINIŲ PLAZMOJE

A. Grigonis [a], Ž. Rutkūnienė [a], M. Šilinskas [b]

[a] *Kauno technologijos universitetas, Kaunas, Lietuva*
[b] *Otto von Guericke universitetas, Magdeburgas, Vokietija*

Santrauka

Amorfinės anglies dangos buvo gaunamos iš $CF_4 + H_2$, C_2H_2, $C_2H_2 + H_2$ ir $C_6H_{14} + H_2$ dujų mišinių. Ėsdinant silicį $CF_4 + H_2$ plazmoje, jo paviršiuje atsiranda sudėtingos sandaros danga iš $(C–CF_x)_n$, $(CH_2)_n$ tipo polimerinių junginių ir α-Si_xC_{1-x}:H:F deimanto tipo anglies (DLC). Raman'o spektroskopija parodė, kad G ir D juostų maksimumai labai pasislinkę mažųjų verčių pusėn, lyginant su kitais būdais gautomis dangomis. Tą poslinkį lemia Si priemaišos, kurių dangoje rasta iki 20%. Polimeriniai junginiai daro dangą porėtą ir minkštą. Didinant apšvitos trukmę, danga storėja, silicio koncentracija mažėja, mikroreljefas ir RS duomenys artėja prie tipinių DLC dangų, gaunamų iš kitų mišinių. Acetileno ir heksano aplinkose dangos buvo nusodinamos ant silicio padėklų tiesioginiu jonų pluošteliu. Naudojant dujinį acetileną galima tiksliai kontroliuoti ir daugiau keisti C_2H_2/H_2 santykį. Dangos, gautos iš C_2H_2/H_2 mišinio, buvo "deimantiškiausios", kai $C_2H_2/H_2 = 1/1$ ir prieš nusodinant dangą Si paviršius 10 min buvo valomas H_2 plazmoje. Jei $C_2H_2/H_2 \geq 1/5$, danga jau nesusidaro. Heksano–vandenilio aplinkoje dangos susidarė vandenilio srautui nunešant nekontroliuojamą C_6H_{14} garų kiekį. Jei į mišinį buvo įterpiamas papildomas vandenilio kiekis, augimo sparta mažėjo, o esant $(C_6H_{14} + H_2) + 3H_2$ danga nesusidarydavo. Susidariusių DLC dangų savybės yra deimantiškiausios, kai papildomo vandenilio nėra (t. y. $C_6H_{14} + H_2$) ir padėklo temperatūra 15 °C.